

The System Design of a Rubidium Maser Frequency Standard

Cheng-Xi Xiong  
Beijing Institute of Radio  
Metrology and Measurement  
Beijing, China

ABSTRACT

The Rubidium Maser Frequency Standard is a precision frequency source with excellent short-term stability. A type PBR-II Rb maser frequency standard has been developed by the Beijing Institute of Radio Metrology and Measurement (BIRMM). The time-domain frequency stability (two-sample variance) of this frequency standard is less than  $1.5 \times 10^{-13} \tau^{-1}$  for  $\tau = 10 \text{ms} \rightarrow 1.0 \text{s}$ ,  $f_0 = 1.0 \text{ kHz}$ .

Two PBR-II frequency standards have been used as reference frequency sources in a frequency stability measurement system.

In this paper some important system characteristics for the PBR-II Rb maser frequency standard such as phase noise and frequency stability transfer characteristics will be discussed. Furthermore, the following topics will be included as well:

1. Design of the frequency standard for optimum frequency stability of the output signal.
2. The choice of a VCXO for the frequency standard.
3. The design of the phase-locked loop.

The frequency stability test results on the PBR-II show the achievement of the system design goals given above.

INTRODUCTION

The Rubidium maser is an active atomic frequency standard. One of its characteristics is that of very good short-term stability. In atomic frequency standards, the Rubidium maser frequency standard has the best frequency stability for averaging times between milliseconds and seconds. Thus, the Rubidium maser is a precision frequency source which can be used in frequency stability measurement systems.

This paper presents the design considerations for the PBR-II rubidium maser frequency standard developed by the Beijing Institute of Radio Metrology and Measurement (BIRMM). The main

problem that will be discussed is the frequency stability of the output signal of the rubidium maser frequency standard. We will first discuss the basic design equations of the frequency standard system and give a description of different phase noise spectral densities occurring in these components so that the relationship between the phase-noise and the frequency stability of the output signal of the frequency standard can be determined. We then discuss the optimization of the design of the low-noise receiver, the VCXO and the phase-locked loop that are used in the PBR-II. Finally we present the methods used and the experimental results for measuring residual frequency instability of the phase-locked receiver. The design values and the experimental values are in basic agreement, demonstrating the validity of the design considerations. A description of the time-domain frequency stability of the complete PBR-II frequency standard and of the Rubidium maser are given.

The Rb maser and the transfer of its frequency stability to an output signal have been discussed extensively (1 through 10). The development of the Rb maser frequency standard began in the BIRMM in 1971. An earlier model of the Rb maser frequency standard which was developed by the Wuhan Institute of Physics and BIRMM has been described before (10). The PBR-II Rb maser frequency standard presented in this paper is a new model. Its frequency stability is now  $1.5 \times 10^{-13} \text{yr}^{-1}$  for averaging times between milliseconds and seconds, and exhibits better operational reliability than the earlier model.

## BASIC SYSTEM DESIGN PRINCIPLES

The system design for the PBR-II was directed toward the achievement of optimum system performance and gives requirements on the various components of the system.

### 1. General Description of the Rb Maser Frequency Standard

The Rubidium maser frequency standard, like other maser atomic frequency standards, consists of a Rb maser and a phase-locked receiver, as shown in Figure 1. The Rb maser is a frequency source with excellent frequency stability. The operating frequency,  $\nu$ , of the maser is 6834 MHz and its power output is on the order of  $10^{-10}$  W. The phase-locked receiver shown in Figure 2 plays a major role in the transfer of the frequency stability to the output signal, conversion to a standard frequency and increase in the power level. A typical system of the Rb maser frequency standard with the relevant components and their contributions are shown in Figure 3. The preamplifier shown in Figure 3 is not used in the PBR-II Rb maser frequency standard. It is included in the diagram for the purpose of analysis and comparison.

The voltage controlled crystal oscillator (VCXO) has a mean output frequency  $\nu_0$ , a phase spectral density  $S_{\phi_0}$  in the locked case and a tuning sensitivity  $K_{\nu}$  expressed in radians/volt-second. Its frequency is multiplied by an integer  $M$  to yield a

signal with frequency  $\nu_{LO1}$  close to the maser frequency. The phase noise contribution of the multiplier referred to the input frequency is given by  $S_{\phi_{Mu}}(f)$ . The microwave mixer is fed by the amplified maser signal (or the maser signal) and the frequency multiplied VCO signal to yield an intermediate frequency (IF) signal with a frequency  $\nu_{IF1}$  much smaller than  $\nu_M$ . The IF contains both the phase instability of the maser and of the multiplied VCO. The VCO signal is also the reference of a frequency of a synthesizer which yields an output frequency  $\nu_{LO3}$  equal to  $\nu_{IF2}$ . The maser frequency, and consequently, the intermediate frequency  $\nu_{IF}$  and the VCO frequency are not related by a simple rational number. The frequency synthesizer acts as a third fractional multiplication factor  $M3$ . The frequency synthesizer also exhibits its own phase noise, but since the multiplication factor is so small it can be neglected when compared to the phase noise added by the first multiplier. The signals with frequencies  $\nu_{IF2}$  and  $\nu_{LO3}$  feed the phase detector having a phase sensitivity  $K_d$  expressed in volts/radian. That part of the receiver comprising the multiplier synthesizer, mixer, IF amplifier and phase detector is designated as the down converter.

The low-frequency output signal of the phase detector is a measure of the phase error between the signals at frequencies  $\nu_M$  and  $\nu_{LO1}$ . The error signal is passed through the loop filter with the transfer function  $F(j\omega)$ . Usually the loop filter is of the low-pass type, and the transfer function is chosen to yield optimal PLL performance. Finally the filtered error signal is fed to the tuning input of the VCO, which is then locked to the frequency of the maser signal.

## 2. Basic Equations

The basic block diagram of the phase-locked system is shown in Figure 2. As stated in (8), the phase noise spectral density of the output of a VCO which is phase-locked to a reference signal can be written:

$$S_{\phi_o}(f) = S_{\phi_x}(f) \cdot |H_1(f)|^2 + S_{\phi_r}(f) \cdot |H_2(f)|^2. \quad (1)$$

The power spectral density of the relative frequency fluctuations can be calculated from:

$$S_{y_o}(f) = (f/\nu_o)^2 \cdot S_{\phi_o}(f) = S_{y_x}(f) \cdot |H_1(f)|^2 + S_{y_r}(f) \cdot |H_2(f)|^2. \quad (2)$$

where

$$H_1(f) = \frac{j2\pi f}{j2\pi f + K_d \cdot K_v \cdot F(j2\pi f)} \quad (3)$$

$$H_2(f) = \frac{K_d \cdot K_v \cdot F(j2\pi f)}{j2\pi f + K_d \cdot K_v \cdot F(j2\pi f)} \quad (4)$$

$H_1(f)$  and  $H_2(f)$  are the transfer functions of the phase locked loop,  $F(j2\pi f)$  is the transfer function of the loop filter,  $K_d$  is

the phase sensitivity of the phase detector,  $K_v$  is the voltage controlled oscillator tuning sensitivity,  $S_{\phi_{rx}}(f)$  and  $S_{\phi_r}(f)$  are the phase noise power spectral density of the free-running VCXO and the reference source respectively.

The above basic relationships can be applied to the Rb maser frequency standard, shown in Figure 3 [11]. The relations for this figure can be expressed:

$$S_{\phi_r}(f) = S_{\phi_{MU}}(f) + (S_{\phi_M}(f) + S_{\phi_1}(f) + S_{\phi_A}(f) + S_{\phi_R}(f) + S_{\phi_{IF1}}(f) + S_{\phi_{R2}}(f) + S_{\phi_2}(f) + S_{\phi_L}(f)) / M^2 + (M_2/M) S_{\phi_{MU2}}(f) + (M_3/M) S_{\phi_S}(f) \quad (5)$$

$$S_{y_r}(f) = S_{y_M}(f) + S_{y_i}(f) + S_{y_A}(f) + S_{y_R}(f) + S_{y_{IF1}}(f) + S_{y_{R2}}(f) + S_{y_{IF2}}(f) + S_{y_1}(f) + S_{y_{MU}}(f) + S_{y_S}(f) \quad (6)$$

$$H_1(f) = \frac{j2\pi f}{j2\pi f + K_d \cdot K_v \cdot M \cdot F(j2\pi f)} \quad (7)$$

$$H_2(f) = \frac{K_d \cdot K_v \cdot M \cdot F(j2\pi f)}{j2\pi f + K_d K_v \cdot M \cdot F(j2\pi f)} \quad (8)$$

$$S_{\phi_o}(f) = S_{\phi_x}(f) \cdot |H_1(f)|^2 + S_{\phi_r}(f) \cdot |H_2(f)|^2 \quad (9)$$

$$S_{y_o}(f) = S_{y_x}(f) \cdot |H_1(f)|^2 + S_{y_r}(f) \cdot |H_2(f)|^2 \quad (10)$$

The time domain frequency stability of the VCXO output signal than then be expressed (12) by:

$$\sigma_{y_o}^2(\tau) = 2 \int_0^{\infty} S_{y_o}(f) \cdot \frac{\sin^4(\pi f \tau)}{(\pi f)^2 \cdot (1 + (f/f_c)^2)} df \quad (11)$$

or

$$\sigma_{y_o}^2(\tau) = \frac{8}{(2\pi V_o \tau)^2} \int_0^{\infty} S_{\phi_o}(f) \cdot \sin^4(\pi f \tau) \cdot \frac{1}{1 + (f/f_c)^2} df \quad (12)$$

where  $f_c$  is the cutoff frequency of the first-order low pass filter used in the measurement system. From equation (10) we see that the first term represents the contribution from the VCXO. The loop acts as a high pass filter with a limiting value of one for very high Fourier frequencies. The second term is the contribution from the reference sources which include the maser, the preamplifier, the mixer the multiplier, etc. In that case, the loop acts as a low pass filter with a limiting value of one for very low Fourier frequencies. The overall performance of the system will then give the high frequency fluctuations of the VCXO plus the low frequency fluctuations of the reference sources. This is an important consideration for the designer of the system.

From the above we can conclude:

1. The reference system consisting of the Rb maser, preamplifier, mixer and multiplier must have low phase noise at low Fourier frequencies. The flicker of phase and flicker of frequency noise must be controlled as low as possible.
2. The VCXO used in the Rubidium maser frequency standard must exhibit very low white phase noise. The long term frequency and drift are not too important.
3. The transfer function  $F(j\omega)$  of the loop filter plays an important role in the frequency standard. The choice of the loop parameters must be made to optimize the frequency stability of the output frequency.

#### CHARACTERIZATION OF THE NOISE IN THE COMPONENTS

##### 1. Rubidium maser

Several authors [9] [11] have shown that the one-sided-spectral density of the fractional frequency fluctuations can be approximated by:

$$S_{YM1}(f) = \frac{4kT}{P_{at}} (f/\nu_M)^2 + \frac{4kT}{P_{at}} (1/2Q_1)^2 \cdot G_c(f) \quad (13)$$

where  $k$  is Boltzmann's constant,  $T$  is the absolute temperature of the system,  $P_{at}$  is the power generated inside the active medium,  $Q_1$  is the atomic line quality factor,  $M$  is the atomic resonant frequency and  $G_c(f)$  is the power transfer function of the microwave cavity. The first term represents the white phase noise contribution and the second term is the white frequency noise contribution resulting from stimulated emission of radiation within the atomic linewidth. According to the experimental results of at BIRMM and the reference [7] there is random walk of frequency in the rubidium maser, but the source of the noise is still unknown. According to the preliminary analysis [3] [6] it is believed to come mainly from cavity temperature fluctuations or light fluctuations. The time domain frequency stability goes as  $\tau^{1/2}$  for averaging time  $\tau > 3s$ . From experimental results, shown in Figure 15, we can obtain  $\sigma_y^2(\tau) = 4.7 \times 10^{-14} \tau^{1/2}$  for  $\tau = 3-100s$ . The power spectral density of the relative frequency fluctuations can be calculated from (12)

$$S_y(f) = \frac{6}{(2\pi)^2 \tau^2} \sigma_y^2(\tau) \quad (14)$$

From (14) we obtain then

$$S_{YM2}(f) = 3.4 \times 10^{-28} f^{-2} \quad (15)$$



The spectral density of fractional frequency fluctuations of the Rb maser FBR-II can be written:

$$S_{yM}(f) = S_{yM1}(f) + S_{yM2}(f) = 3.4 \times 10^{-28} f^{-2} + 2.5 \times 10^{-27} + 2 \times 10^{-30} f^2 \quad (16)$$

Thus, the power spectral density of the phase noise can be expressed:

$$S_{\phi}(f) = (2\pi f)^2 S_{yM}(f) = 10^{-7.8} f^{-4} + 10^{-6.9} f^{-2} + 10^{-10} \quad (17)$$

### 2. VCXO

VCXOs which are commonly used with atomic frequency standards are 5MHz, 10 MHz and 100MHz quartz crystal oscillators. The power spectral density of the phase noise of the VCXOs which have been developed at BIRM can be expressed as:

$$S_{\phi,1}(f) = 10^{-10} f^{-3} + 10^{-11} f^{-1} + 10^{-15} \quad (5\text{MHz VCXO}) \quad (18)$$

$$S_{\phi,2}(f) = 10^{-9} f^{-3} + 10^{-10.2} f^{-1} + 10^{-15} \quad (10\text{MHz VCXO}) \quad (19)$$

$$S_{\phi,3}(f) = 10^{-5} f^{-3} + 10^{-15} \quad (100\text{MHz VCXO}) \quad (20)$$

The power spectral density of the fractional frequency fluctuations can then be written:

$$S_{y,1}(f) = 4 \times 10^{-24} f^{-1} + 4 \times 10^{-25} f + 4 \times 10^{-29} f^2 \quad (5\text{MHz VCXO}) \quad (21)$$

$$S_{y,2}(f) = 10^{-23} f^{-1} + 5.3 \times 10^{-25} f + 10^{-29} f^2 \quad (10\text{MHz VCXO}) \quad (22)$$

$$S_{y,3}(f) = 10^{-21} f^{-1} + 10^{-31} f^2 \quad (100\text{MHz VCXO}) \quad (23)$$

### 3. Microwave preamplifier

Microwave preamplifiers find wide use in low-noise receivers, so we have been trying to find a suitable unit for Rubidium maser use. We have only been able to find FET microwave amplifiers. The phase noise of several of these amplifiers were tested. Models CX511A and CX511C are being used in the Rb maser. They have a gain of 17.2 to 17.5 dB and a noise figure of 4 to 6 dB over an input power range of -20 to -60 dBm. The phase noise spectral density was found to be:

$$S_{\phi A}(f) = (10^{-17.1 \sim 6.1}) f^{-3} + (10^{-8.3 \sim 9.3}) f^{-1} + (10^{-19.7 \sim 20.1}) P_i^{-1} \quad (24)$$

where  $P_i$  is the input power level, expressed in watts. Equation (24) shows that the FET amplifier has not only white phase noise, but also flicker FM and PM noise. The first term represents the flicker FM noise, the second term represents the flicker PM noise. They are independent of the input signal power level for an typical amplifier. The noise level varies with the FET model and the operational conditions of the amplifier. The third term represents white phase noise. This noise is independent of the input signal power level and amplifier noise figure.



ORIGINAL PAGE IS  
OF POOR QUALITY

From (24), the spectral density of fractional frequency fluctuation can be written:

$$S_{Y_a}(f) = (1.7-17) \times 10^{-26} f^{-1} + (1-10) \times 10^{-29} f + (1.7-4.3) \times 10^{-40} f^2 P_i^{-1} \quad (25)$$

Data on flicker PM and flicker FM noise levels of such an amplifier are not available from any source to our knowledge. We will make a further effort to develop low noise preamplifiers in the future.

#### 4. Microwave Mixer

The microwave mixer is an important component in the PBR-II frequency standard. The white phase noise of a mixer which operates at low signal level is available from the noise figure specification. Data on flicker PM noise at low signal levels are not available and must be measured. The phase noise of several microwave low level balanced mixers have been measured. The model WH32 Schottky diodes are used in the mixer.

The mixer has a noise figure of 6-10 dB, a LO power  $P_l$  of 3 dBm and signal power level of 0 dBm to -20 dBm.

The phase noise spectral density is found to be:

$$S_{\phi R}(f) = (10^{-15.2-16.2}) f^{-1} P_s^{-1} + (10^{-18.2-19.2}) P_s^{-1} \quad (26)$$

where  $P_s$  is the signal power level expressed in watts.

The local oscillator power to the mixer is constant, so that the operating condition of the mixer is invariant. We can deduce a conclusion from the above statements that expression (26) will be valid for lower signal levels. From (26), the spectral density of fractional frequency fluctuations of the mixer can be written as:

$$S_{Y R}(f) = (13.5) \times 10^{-36} f P_s^{-1} + (1.35-13.5) \times 10^{-39} f^2 P_s^{-1} \quad (27)$$

According to (27), the phase noise of the mixer is in inverse proportion to the signal power level for the case of low signal levels. The first term represents flicker PM noise which was neglected in general. The second term represents white phase noise which is dependent on the noise figure of the mixer. The phase noise varies with the diode and the microwave circuit of the mixer.

#### 5. Microwave frequency multiplier

The frequency multiplier consists of a transistor power amplifier, a 100 MHz frequency doubler and a high order multiplier with a step recovery diode. The input power is 0 dBm and the output power is +13 dBm at 6.8 GHz. The measured phase noise spectral density referred to 100 MHz is:

$$S_{\phi MU}(f) = 10^{-11} f^{-1} + 10^{-15}$$

The spectral density of the fractional frequency fluctuations can be given:

$$S_{YMU}(f) = 10^{-17}f + 10^{-31}f^2 \quad (28)$$

#### 6. Microwave isolator and attenuator

The isolator and attenuator are passive dissipative non-reciprocal components and contribute only white phase noise:

$$S_{\phi_i}(f) = \frac{(1-\alpha)KT}{\alpha P_i} \quad (29)$$

where  $\alpha$  is the insertion loss of the isolator and attenuator and  $P_i$  is the available signal power at the input of the components. The actual values are:  $P_i = 1 \times 10^{-10} \text{ W}$ ,  $\alpha = 0.8$  (1 dB). From (27) it follows that:

$$S_{\phi_i}(f) = 10^{-10.28} \quad (30)$$

and

$$S_{Y_1}(f) = 10^{-30}f^2 \quad (31)$$

#### 7. Other components in receiver

The influence of the other components in the receiver on the performance of the frequency standard is theoretically smaller than that of the above components. In order to improve the performance of the frequency standard, we measure phase noise and frequency stability of these components to acquire the following results:

##### a. 5 MHz x 7 frequency multiplier

$$S_{\phi MU2}(f) = 10^{-12}f^{-1} + 10^{-15} \quad (32)$$

##### b. Phase detector

$$S_{\phi p}(f) = 10^{-12.5}f^{-1} + 10^{-15.5} \quad (33)$$

##### c. Second mixer

$$S_{\phi R2}(f) = 10^{-12.5}f^{-1} + 10^{-15.7} \quad (34)$$

##### d. Frequency synthesizer

$$\sigma_{Y_S}(\tau) \leq 1 \times 10^{-9}f^{-1} \quad \text{for } f_h = 1 \text{ kHz} \quad (35)$$

Therefore:

$$S_{YMU2}(f) = 4 \times 10^{-26}f + 4 \times 10^{-30}f^2 \quad (36)$$

$$S_{Y_0}(f) = 6.8 \times 10^{-33}f + 6.8 \times 10^{-36}f^2 \quad (37)$$

$$S_{YR2}(f) = 6.8 \times 10^{-33}f + 4.3 \times 10^{-36}f^2 \quad (38)$$

## 8. Summary of the noise contributions

In order to compare the noise contributions of the different components, the power spectral density of fractional frequency fluctuation of the various components are given in Figure 4.

### CONSIDERATIONS OF THE SYSTEM DESIGN

By system design we mean the optimization of the system frequency stability. In this section we will present design considerations of the main components in the PBR-II frequency standard.

#### 1. Consideration of the Rubidium maser design

From (16), the output signal of the Rb maser exhibits three main noise components. Because the Rb maser is included in the reference source of the frequency standard, the noise contribution of the low Fourier frequencies is the main contribution to the output frequency of the frequency standard. We see from Figure (4) that the main noise component is random walk FM. Other noise components can be neglected compared to the flicker phase noise of the microwave mixer of the reference source system.

In order to reduce the random walk FM noise, a high precision DC power supply and high stability oven are used in the PBR-II. Even then a good method has not been found to reduce this noise component.

According to (27), it is very important to increase the output power of the Rb maser to reduce the noise contribution of the microwave mixer. With this end in view, the microwave cavity and the maser bulb operate at a temperature of  $60^{\circ}\text{C}-62^{\circ}\text{C}$ . The lamp oscillator can give an output power of about 10 W. Thus, the output power of the Rb maser is on the order of  $2 \times 10^{-10}$  W. A detailed design of the maser will not be given in this paper.

#### 2. Low noise receiver

Generally a low noise microwave receiver is characterized by the noise figure, but only the white phase noise can be determined by this value.

As stated above, the FET preamplifier and the microwave mixer exhibit flicker FM or FM noise in addition to white phase noise. They will contribute to the overall noise of the frequency standard and degrade the performance.

There two methods which could be used to receive the low power level output of the Rb maser. One of these uses a FET preamplifier and the other goes directly into the microwave mixer. The noise contribution of each method is given in Figures 5a and 5b, where  $S_{yRe1}(f)$ ,  $S_{yRe2}(f)$ ,  $\sigma_{yRe1}(\tau)$  and  $\sigma_{yRe2}(\tau)$  represent the frequency domain and time domain noise contribution of the first and second method.

Assuming that other noise contributions can be neglected compared to the preamplifier and microwave mixer, the noise contribution of each method can be expressed:

$$S_{yRe1}(f) = S_{ya}(f) \quad (39)$$

$$S_{yRe2}(f) = S_{yR}(f) \quad (40)$$

and consequently

$$\sigma_{yRe1}(\tau) = 2 \int_0^{\infty} S_{ya}(f) \frac{\sin^4(\pi\tau f)}{(\pi\tau f)^2(1+(f/f_c)^2)} df \quad (41)$$

$$\sigma_{yRe2}(\tau) = 2 \int_0^{\infty} S_{yR}(f) \frac{\sin^4(\pi\tau f)}{(\pi\tau f)^2(1+(f/f_c)^2)} df \quad (42)$$

From Figures 5a and 5b, we see that: the second method is better than the first, that is, the noise contribution of the microwave mixer is less than the FET amplifier. In view of operational reliability, noise contribution, cost and volume of the system, we have decided to choose the system with the microwave mixer as the input stage of the phase-locked receiver.

### 3. Choice of VCXO

The VCXO is an important component in the active frequency standard. It must be locked to the resonant frequency of the atomic line and exhibit excellent spectral purity and low white phase noise.

The 100 MHz VCXO has been chosen as the basic oscillator in the PRB-II Rb maser frequency standard. The reasons are summarized below:

(1) In view of the noise contribution for frequency stability of the system, the white phase noise of the VCXO is most important. From Figure 4, we can see that the white phase noise of the 100 MHz VCXO is less than the 10 MHz VCXO and the 5 MHz VCXO.

The Rb maser frequency standard using the 5 MHz VCXO has been discussed extensively in references [7] and [8]. It has been shown that the 5 MHz VCXO is not the best choice for the Rb maser frequency standard.

(2) The order of the frequency multiplier will be reduced with respect to the 5 MHz VCXO and 10 MHz VCXO. The noise contribution of the frequency multipliers will be thus reduced and the stability of the multiplier chain can be improved.

The frequency multiplier has an input frequency of 5 MHz and an output frequency of 6800 MHz. The measured phase noise spectral density, referred to 5 MHz is

$$S_{\phi MU}(f) = 10^{-12} f^{-1} + 10^{-15.7} \quad (43)$$

and

ORIGINAL PAGE IS  
OF POOR QUALITY

$$S_{\text{MU}}(f) = 4 \times 10^{-26} f + 8 \times 10^{-30} f^2 \quad (44)$$

The noise contribution of the frequency multiplier chain with an input of 5 MHz will become a major factor in degrading the frequency stability of the reference source system in the Rb maser frequency standard.

(3) The PBR-II frequency standard is mainly used as a reference frequency source with excellent frequency stability in the measurement of short-term frequency stability. The high stability precision frequency sources, such as 5 MHz and 10 MHz standards must be multiplied to 100 MHz to achieve sufficient measurement resolution. The PBR-II output need not be multiplied, thereby improving the performance of the measuring system.

#### (4) Design of the phase-locked loop

The main task of the loop is to correct the frequency drift of the VCXO and to transfer the frequency stability of the Rb maser to the output. Doubly balanced mixers using Schottky diodes are used as the phase detector which has to be very sensitive and contribute very little noise. In order that no frequency error exists when the free-running VCXO is drifting, a second order loop type 2 [13] is chosen. An integrator with phase-lead correction gives rather good loop stability performance and is used as a filter following the phase detector. Its transfer function is:

$$F(j\omega) = \frac{1 + j\omega\tau_2}{j\omega\tau_1} \quad (45)$$

After substitution of (45) into (7) and (8), the two loop transfer functions become

$$H_1(s) = \frac{\xi^2}{s^2 + 2\xi\omega_n s + \omega_n^2} \quad (46)$$

$$H_2(s) = \frac{2\xi\omega_n s + \omega_n^2}{s^2 + 2\xi\omega_n s + \omega_n^2} \quad (47)$$

where  $s = j\omega$ ,  $\omega_n$  is the natural frequency of the loop and is defined by  $\omega_n = 2\pi f_n = (K_d K_v M / \tau_1)^{1/2}$  (48) and  $\xi$  is the damping factor defined by:

$$\xi = \frac{\omega_n \tau_2}{2} = \frac{Z_2}{2} \cdot \frac{(K_d K_v M)^{1/2}}{\tau_1^{1/2}} \quad (49)$$

With this loop design these two parameters  $\xi$  and  $\omega_n$  can be selected independently by setting the values of  $\tau_1$  and  $\tau_2$

is important when one is concerned with the conditions for optimum transfer of frequency stability.

The capture and locking range are not critical parameters in the active atomic frequency standard, because the two frequencies are already very close to each other and stable.

From the expressions (46) and (47), the transfer functions of the frequency standard system can be written:

$$|H_1(f)|^2 = \frac{f^4}{f^4 + 2f_n^2(2\xi^2 - 1)f^2 + f_n^4} \quad (50)$$

$$|H_2(f)|^2 = \frac{f_n^2(4\xi^2 f^2 + f_n^2)}{f^4 + 2f_n^2(2\xi^2 - 1)f^2 + f_n^4} \quad (51)$$

When  $\xi = 0.707$ , that is the critical damping, (50) and (51) can be written:

$$|H_1(f)|^2 = \frac{f^4}{f^4 + f_n^4} \quad (52)$$

$$|H_2(f)|^2 = \frac{f_n^4 + 2f_n^2 f^2}{f^4 + f_n^4} \quad (53)$$

When  $f/f_n = 1.55$ , these two transfer functions are equal. The first method of loop design for the PBR-II is a method of rough approximation of  $f_n$  and calculation of the values of  $\tau_1$  and  $\tau_2$  according to the equations:

$$\tau_1 = \frac{k_d K_v M}{\omega_n^2} \quad (54)$$

$$\tau_2 = \frac{2\xi}{\omega_n} \quad (55)$$

If the cross-over point of power spectral density of fractional frequency fluctuation between the 100 MHz VCXO and the reference source can be found, such as point O in Figure 4, denote the frequency of the cross-over point by  $f_o$  and the natural frequency of the loop can be expressed as:

$$f_n = \frac{f_o}{1.55} \quad (56)$$

Another method of loop design which has been applied to the PBR-II frequency standard is the calculation of  $f_n$  from the optimum frequency stability of the output signal. A microcomputer was

ORIGINAL PAGE IS  
OF POOR QUALITY

used to calculate the optimum value of  $f_n$  according to the expression (11) or (12). For example, according to the first method, we find  $f_0 = 170$  Hz from Figure 4. Then,  $f_n$  is obtained:

$$f_n = \frac{f_0}{1.55} = 110 \text{ Hz}$$

The values of  $\tau_1$  and  $\tau_2$  can be evaluated from (54) and (55)

$$\tau_1 = \frac{k_d K_v M}{\omega_n^2} = 15 \text{ ms}$$

$$\tau_2 = \frac{2\zeta}{\omega_n} = 2.2 \text{ ms}$$

where  $k_d = 0.5$  v/rad,  $K_v = 30 \times 2\pi$  rad/v,  $M = 68$ ,  $\zeta = 0.707$  and  $\omega_n = 2 \times 110\pi$  rad/s. The actual values of  $\tau_1$  and  $\tau_2$  will be determined by setting the value of  $R$  while measuring the frequency stability of the PBR-II frequency standard.

#### DESCRIPTION OF THE SYSTEM BLOCK DIAGRAM

The system block diagram of the PBR-II frequency standard is shown in Figure 17. The microwave mixer is used as the first stage of the phase-locked receiver and a 100 MHz VCXO is used as the basic oscillator. The second LO signal of 35 MHz is delivered from a 5 MHz VCXO used as a reference signal for the 311 kHz frequency synthesizer. The 5 MHz signal is a non-standard output signal. Its noise contribution can be neglected compared to the 100 MHz VCXO. We can show that the time-domain frequency stability which is added by the 5 MHz VCXO can be expressed as:

$$\sigma_{y_0}^{-1}(\tau) = (35/6800)\sigma_{y_5}(\tau) \quad (57)$$

where  $\sigma_{y_0}^{-1}(\tau)$  is the time domain frequency stability added by the 5 MHz VCXO and  $\sigma_{y_5}(\tau)$  is the time-domain frequency stability of the 5 MHz VCXO. From (57)  $\sigma_{y_0}^{-1}(\tau) = 5 \times 10^{-14} \tau^{-1}$  for  $\sigma_{y_5}(\tau) = 1 \times 10^{-11} \tau^{-1}$ . The 5 MHz VCXO is readily available from our own laboratory. It can also be operated open loop if the frequency stability of the free-running VCXO is good enough for the system. The 311 kHz frequency synthesizer has a frequency range of 1 kHz and a resolution of 1 Hz. It has a time-domain frequency stability better than  $1 \times 10^{-9} \tau^{-1}$ . A 311 kHz quartz crystal oscillator may be substituted for the synthesizer for less demanding uses.

#### PERFORMANCE EVALUATION

The time-domain frequency stability is a most important specification of the PBR-II frequency standard. The basic equations for evaluating the time-domain frequency stability of the output signal of the frequency standard can be written as:

$$\sigma_{y_0}^2(\tau) = 2 \int_0^{\infty} S_{y_0}(f) \frac{\sin^4(\pi\tau f)}{(\pi\tau f)^2 (1+(f/f_c)^2)} df \quad (58)$$

$$S_{y_0}(f) = S_{y_x}(f) |H_1(f)|^2 + S_{y_r} |H_2(f)|^2 \quad (59)$$

$$S_{y_r}(f) = S_{y_m}(f) + S_{y_r}(f) + S_{y_{MU}}(f) \quad (60)$$

$$|H_1(f)|^2 = \frac{f^4}{f^4 + f_n^4} \quad (61)$$

$$|H_2(f)|^2 = \frac{f^4 + 2f_n^2 f^2}{f^4 + f_n^4} \quad (62)$$

The spectral density of fractional frequency fluctuation of the main components in the PBR-II is found to be

$$S_{y_m}(f) = 3.34 \times 10^{-28} f^{-2} + 2.5 \times 10^{-27} + 2 \times 10^{-10} f^2 \quad (63)$$

$$S_{y_r}(f) = 2.1 \times 10^{-26} f + 1.0 \times 10^{-28} f^2 \quad (64)$$

$$S_{y_{MU}}(f) = 1.0 \times 10^{-27} f + 1.0 \times 10^{-31} f^2 \quad (65)$$

$$S_{y_x}(f) = 1.0 \times 10^{-21} f + 1.0 \times 10^{-31} f^2 \quad (66)$$

After substitution of (63)-(65)-(66), the numerical evaluation of  $\sigma_{y_0}(\tau)$  from (58) can be obtained. It is shown in Figure 6 for cutoff frequency  $f_c = 1$  kHz and a loop natural frequency of  $f_n = 200$  Hz. We see that  $\sigma_{y_0}(\tau)$  shows a  $\tau^{-1}$  dependence over the range of averaging times from 2 ms to 1 s and a  $\tau^{0.5}$  dependence for averaging times  $\tau > 3$  s. According to Figure 6, the time domain frequency stability  $\sigma_{y_0}(\tau)$  can be expressed approximately as

$$\sigma_{y_0}(\tau) = [(1.4 \times 10^{-13} \tau^{-1})^2 + (4.7 \times 10^{-14} \tau^{0.5})^2]^{0.5} \quad (67)$$

From the second design method, we evaluated the optimum value of  $f_n$ . The relationship between the numerical evaluation of  $\sigma_{y_0}(0.1 \text{ s})$  and the natural frequency of the loop is shown in Figure 7. It is seen that the optimum value of  $f_n$  is about 180 Hz.

## EXPERIMENTAL RESULTS

### 1. Time domain frequency stability

The time domain frequency stability (two-sample variance) of the PBR-II frequency standard was measured using the configuration shown in Figures 8 and 9. The results are given in Figure 10.

The beat frequency method is used as the basic frequency stability measurement method. For averaging times between 2 ms and

ORIGINAL PAGE IS  
OF POOR QUALITY

100 ms, the reference oscillator is a low-noise frequency synthesizer. The beat frequency is approximately 10 Hz-500 Hz. For averaging times from 100 ms -100s, the reference oscillator is another PBR-II frequency standard. The beat frequency is about 10 Hz. The noise bandwidth is about 1 kHz for averaging times between 2 ms and 100 s.

### 2. Frequency instability added by the phase-locked receiver

The frequency instability added by the phase-locked receiver is defined as the frequency stability of the output signal of the Rb maser frequency standard when the Rb maser is an ideal oscillator, that is,  $S_{YM}(f)=0$ . A detailed block diagram of the measurement system is shown in Figure 11a and 11b. The measurement principle is shown in Figure 12a and 12b.

The noise spectral density shown in Figure 12a can be written as:

$$\begin{aligned}
 S_{Y0}(f) = & S_{YX}(f) |H_1(f)|_L^2 + S_{YR}(f) |H_2(f)|_L^2 + \\
 & S_{YUX}(f) |H_1(f)|_S^2 |H_2(f)|^2 + \\
 & S_{Y01} [1 - |H_2(f)|_S^2 |H_2(f)|^2] + \\
 & S_{YS}(f) |H_2(f)|_S^4 |H_2(f)|_L^2 \quad (68)
 \end{aligned}$$

where  $|H(f)|_S^2$  and  $|H(f)|_L^2$  are respectively the system transfer functions of the microwave synthesizer and the phase-locked receiver.  $S_{YUX}(f)$  and  $S_{YU0}(f)$  represent the noise spectral density of the VCXO in free oscillation and locked condition respectively,  $S_{YX}(f)$  represents the noise spectral density of the 100 MHz VCXO of the receiver in free oscillation,  $S_{Y01}(f)$  represents the noise spectral density of the 100 MHz VCXO in the microwave synthesizer,  $S_{YS}(f)$  and  $S_{YR}(f)$  represent the noise contributions of the synthesizer and the phase-locked receiver reference system respectively and  $S_{Yp1}(f)$  is the noise contribution of the phase-locked receiver. Because the phase lock bandwidth of the synthesizer is wider than the receiver's, the fourth term in (51) can be neglected. The third and fifth terms can be measured by the method shown in Figure 11b. The first and second terms in (68) can be evaluated by

$$S_{Yp1}(f) = S_{YX} |H_1(f)|_L^2 + S_{YR}(f) |H_2(f)|_L^2.$$

The time domain frequency instability added by the phase-locked receiver is measured actually by the beat frequency method. The beat frequency signal between two 100 MHz VCXO's is about 10 Hz to 100 Hz, which can be obtained by varying the output frequency of the microwave synthesizer. The measurement results are shown in Figure 13.

### 3. Rubidium maser

The block diagram of the measurement setup is shown in Figure 13. Shown in Figure 15 is the measurement result which includes the

noise contribution of the receiver. We have not found a good method to precisely measure the noise contribution of the Rb maser.

The beat frequency signal between the two Rb masers is about 500 Hz. The twin-T tuned amplifier is used to control the noise bandwidth from 3 Hz to 3 kHz.

#### 4. Discussion

From the measurement results in Figures 10 through 15, we see that the noise contribution of the phase-locked receiver predominates for  $2 \text{ ms} \leq \tau \leq 1 \text{ s}$ . For longer averaging times the random walk FM noise of the Rb maser predominates and degrades the frequency stability of the PBR-II frequency standard.

The measurement results of Figure 16 basically agrees with the calculated values.

The frequer. instability added by the phase-locked receiver can be used to characterize the performance of the receiver. It is very useful for developing a low-noise phase-locked receiver. From the measurement results in Figure 15, we see that  $\sigma_y(\tau)$  shows a  $[1.038 + 3\text{Ln}(2\pi f_n \tau)]^{1/2}$  dependence over the range of averaging times from 10 ms to 1 s for noise bandwidths,  $f_n$ , from 10 Hz to 1 kHz. This dependence shows clearly that the noise contribution of  $1/f$  PM noise of the microwave mixer predominates for  $10 \text{ ms} \leq \tau \leq 1 \text{ s}$ .

#### Conclusion

We have shown that the system design method adopted for the PBR-II maser frequency standard is a useful one for choosing components and parameter design. Precision characterization of the noise spectral density is the basis of the system design. The main noise contribution from the PBR-II frequency standard is the flicker phase noise of the microwave mixer, random walk FM noise of the the Rb maser and white phase noise of the 100 MHz VCXO.

#### Acknowledgment

The author wishes to acknowledge the helpful assistance of the Wuhan Institute of Physics in the development of the Rubidium maser.

The author also is indebted to Prof. Qiao and Mr. Xie for their assistance in the preparation of the manuscript.

## REFERENCES

- (1) P. Davidovits and R. Novick., "The optically pumped rubidium maser" Proc IEEE. Vol.54 pp.155-170 1966.
- (2) J. Vanier., "Relaxation in Rb<sup>87</sup> and the rubidium maser" Phys Rev. Vol.168 pp.129-149 1968.
- (3) E.N. Bazarov. V.P. Goubin., "Short-term frequency stability of Rb maser". Trans IEEE IM-19 No4 pp.417-419 1970
- (4) M. Tetu, G. Busca and J. Vanier., "Short-term frequency stability of the Rb<sup>87</sup> maser" IEEE Trans Instrum. Meas. Vol. IM-22 pp.250-257 1973.
- (5) G. Busca. R. Brousseau and J. Vanier "Long-term frequency stability of the Rb<sup>87</sup> maser". IEEE Trans Instrum. Meas Vol. IM-24 pp.291-296 1975.
- (6) J. Vanier. M. Tetu and L. G. Bernier. "Transfer of frequency stability from an atomic frequency reference to a quartz crystal oscillator" IEEE Trans. Instrum. Meas. Vol. IM-28 pp.188-193 1979.
- (7) M. Tetu. R. Brousseau and J. Vanier. "Frequency domain measurements of the frequency stability of a maser oscillator" IEEE Trans. Instrum. Meas. Vol. IM-29. pp.94- 1980.
- (8) J. Vanier and M. Tetu., "Phase-locked loops used with masers: atomic frequency standards". IEEE Trans. Communications. Vol. COM-30 No.10 pp.2355-2361 1982.
- (9) M. Tetu. P. Tremblay. D. Bonnier. and J. Vanier. "Short-term frequency stability and systematic effects on the rubidium 87 maser oscillator frequency". Proc of the 36th Annual Symposium

on Frequency Control 1982. pp.340-347.

(10) H. T. Wang. "The frequency and time standard and activities at the Beijing Institute of Radio Metrology and Measurements" Proc 11th Annual PTTI 1979. pp.657.

(11) L. S. Cutler and C.L. Searle., "Some aspects of the theory and measurements of frequency fluctuations in frequency standards" Proc IEEE Vol. 54 pp.136-154 1966.

(12) J. A. Barnes. et al., "Characterization of frequency stability" IEEE Trans. Instrum. Meas. Vol. IM-20. pp.105-120. 1971.

(13) F. M. Gardner., Phaselock Technigues JOHN WILEY & SONES. 1979.

ORIGINAL PAGE IS  
OF POOR QUALITY

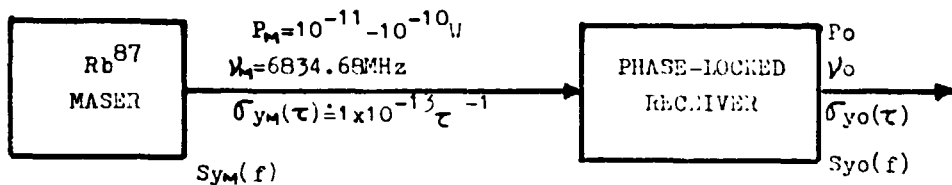


Fig.1. Basic configuration of Rb maser frequency standard

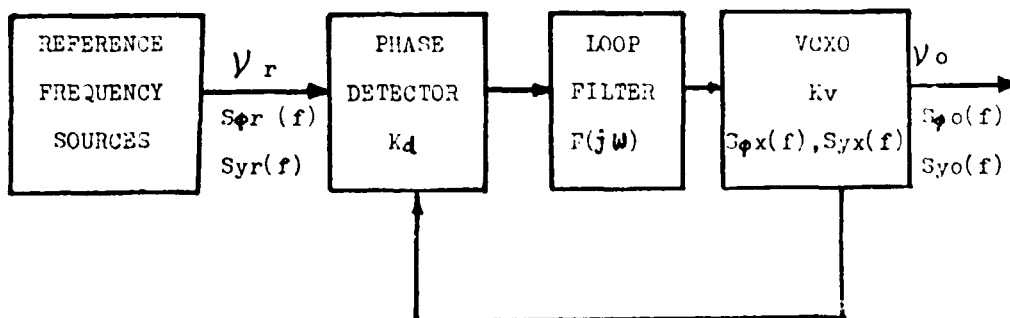


Fig.2. Basic block diagram of phase-locked system

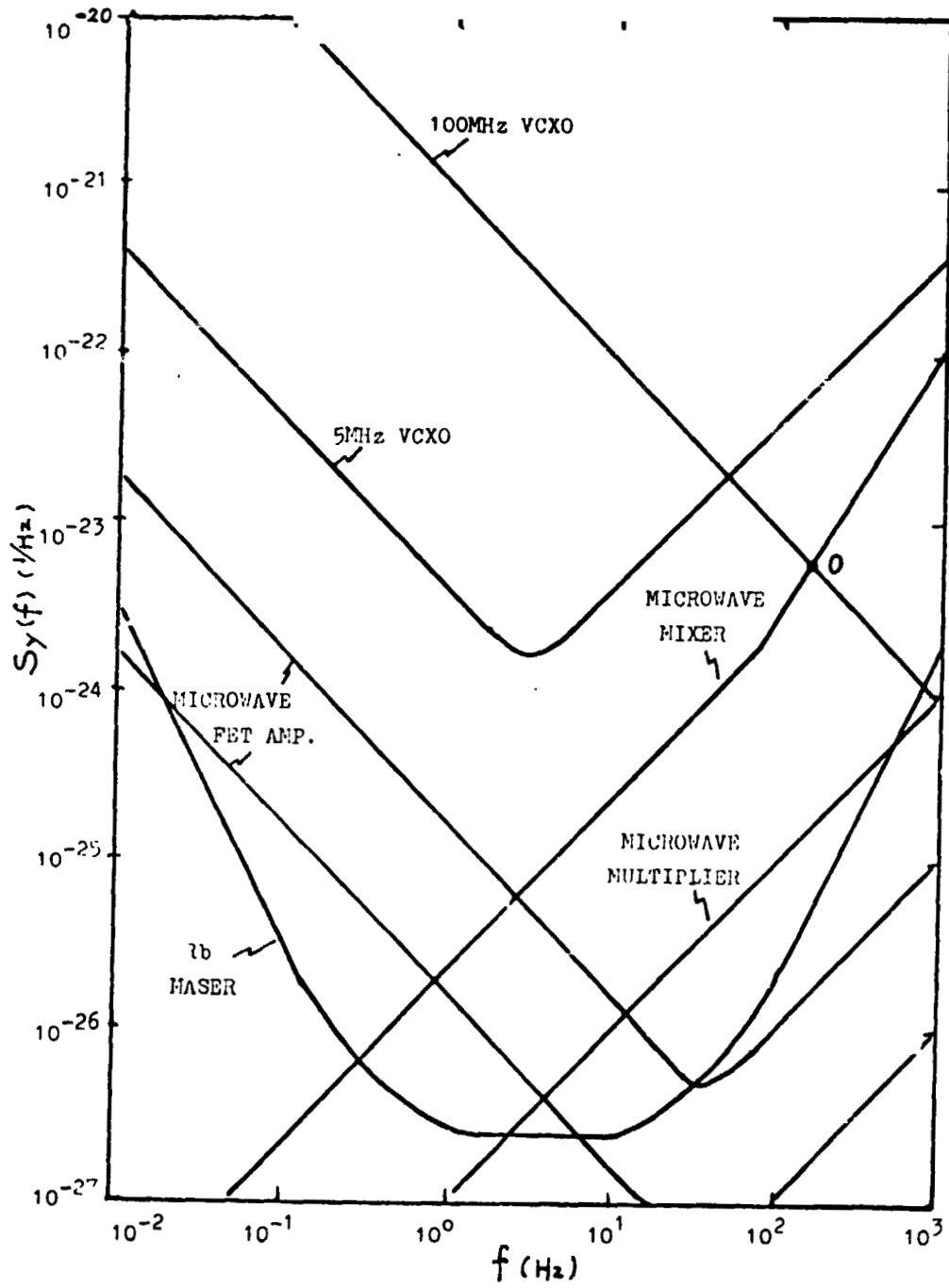


Fig.4. Frequency-domain stability of main components

ORIGINAL PAGE IS  
OF POOR QUALITY

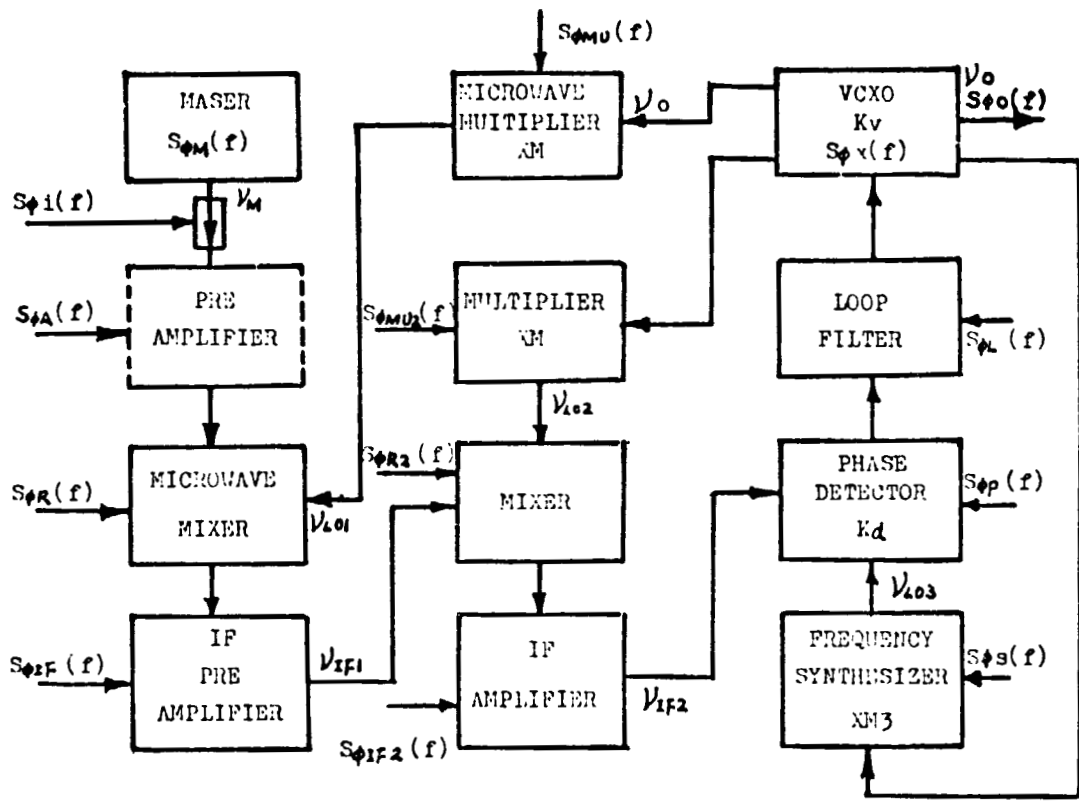


Fig. 3. General block diagram of a maser receiver and main  
noise contribution

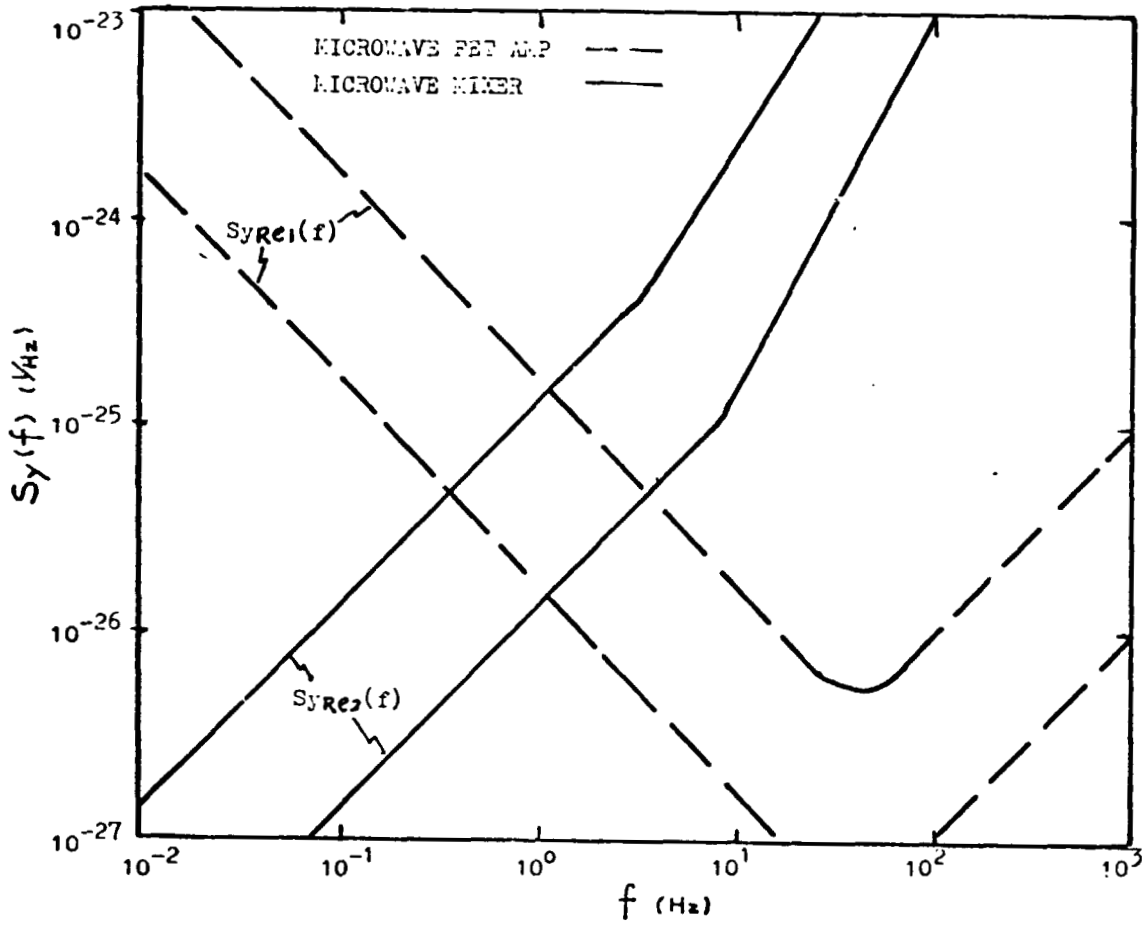


Fig. 5, a Frequency-domain frequency stability of two low-noise receives.

ORIGINAL PACE IS  
OF POOR QUALITY

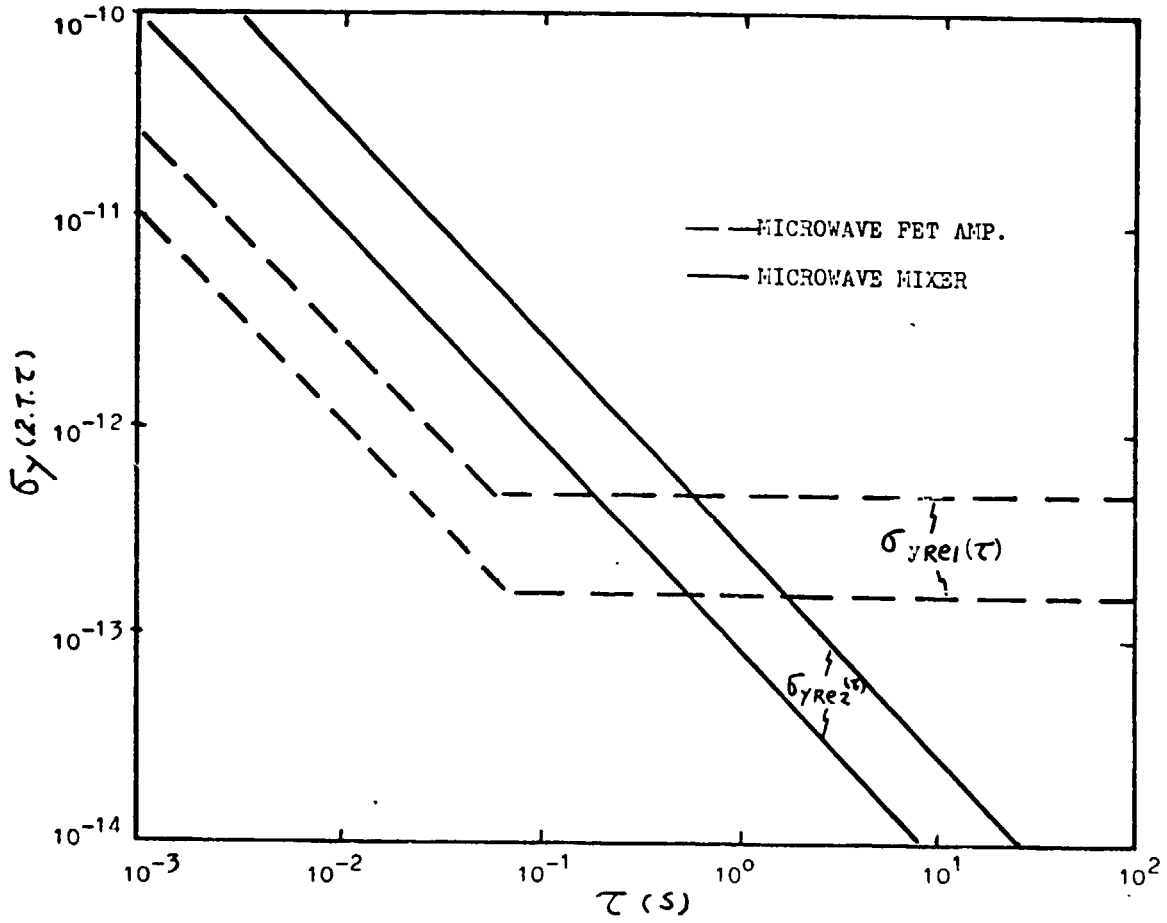


Fig. 5.b Time-domain frequency stability of two low-noise receives.

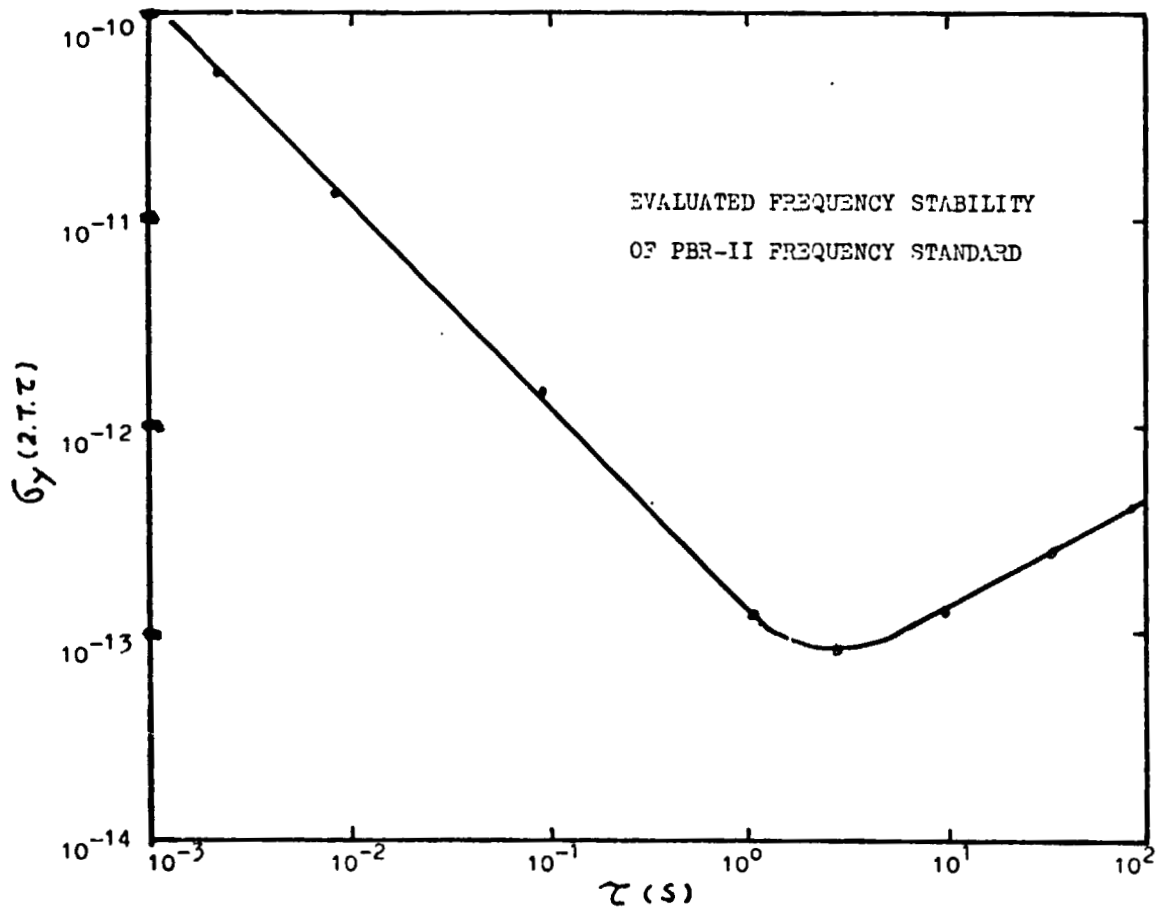


Fig.6. Evaluated time-domain frequency stability of PBR-II

ORIGINAL PAGE IS  
OF POOR QUALITY

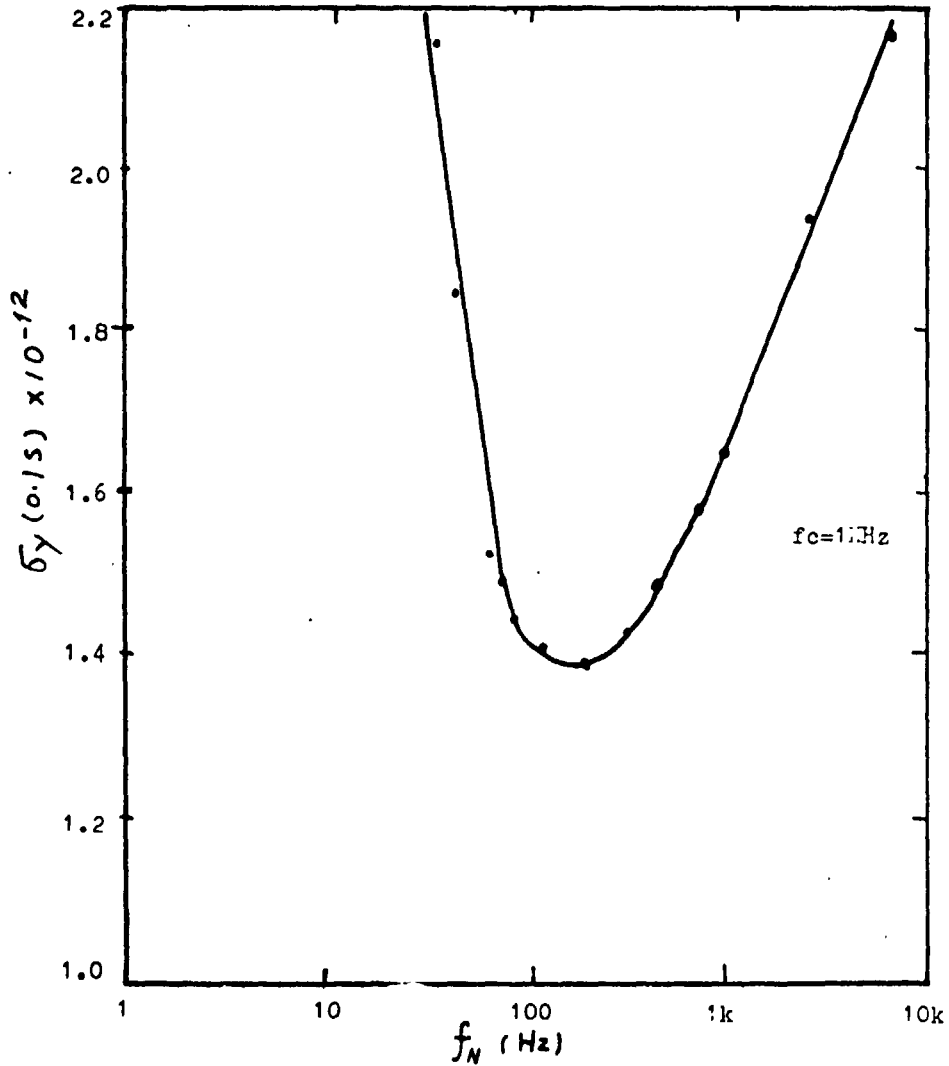


Fig.7. Evaluated value of the time-domain frequency stability  $\sigma_y(0.1s)$  versus loop nature frequency  $f_N$  for  $\tau = 0.1^s$ ,  $f_c = 1 \text{ kHz}$ .

ORIGINAL PAGE IS  
OF POOR QUALITY

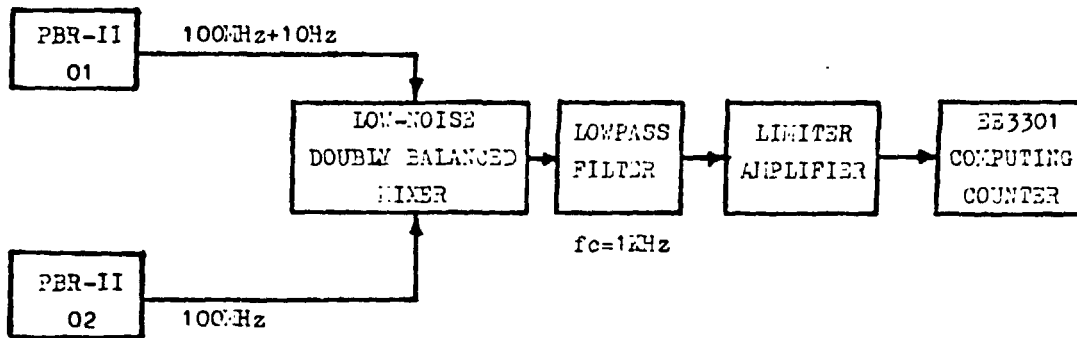


Fig.8. Experimental setup used in measurement of PBR-II frequency stability for averaging time  $\tau = 100^{\text{ms}} - 100^{\text{s}}$ .

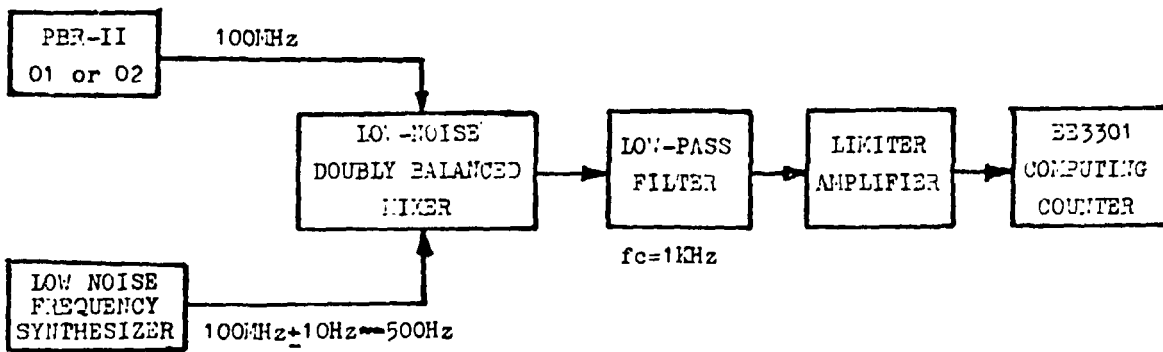


Fig.9. Experimental setup used in measurement of PBR-II frequency stability for averaging time  $\tau = 2^{\text{ms}} - 100^{\text{ms}}$ .

ORIGINAL PAGE IS  
OF POOR QUALITY

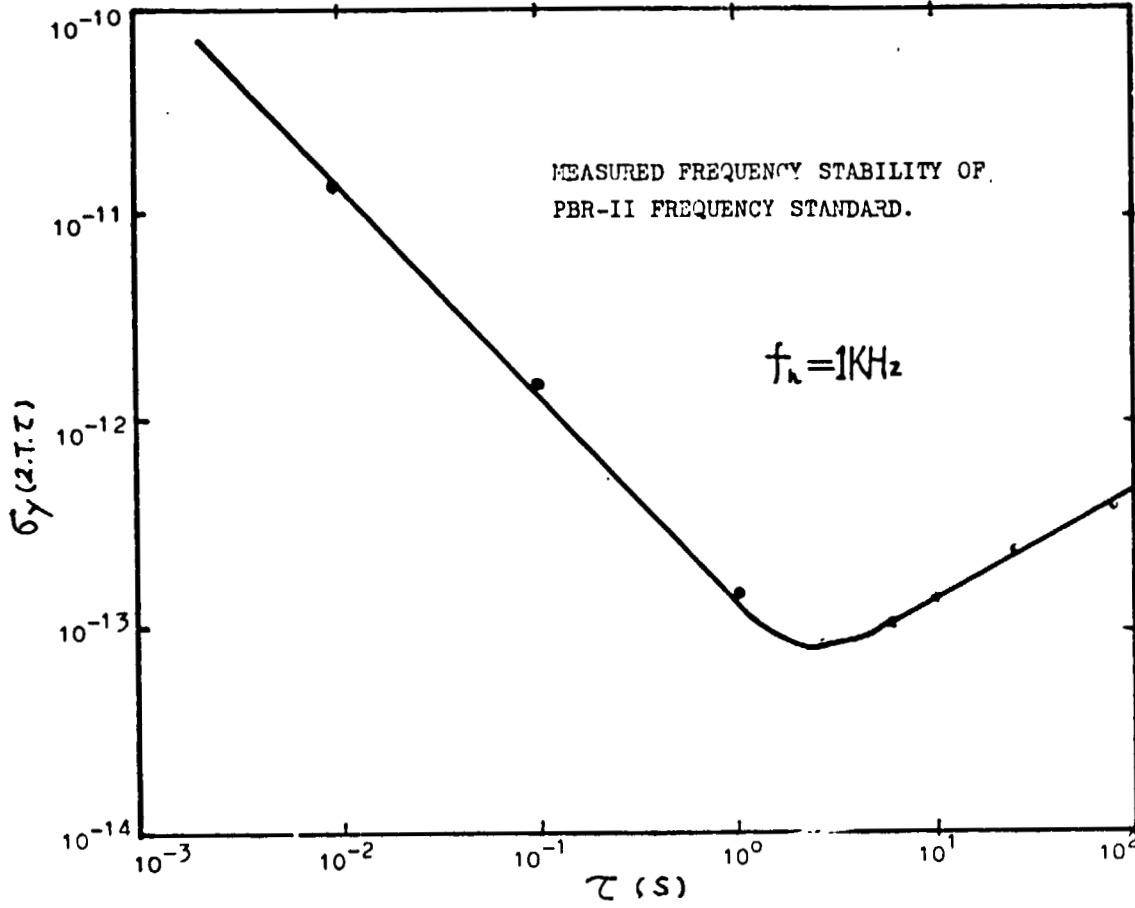
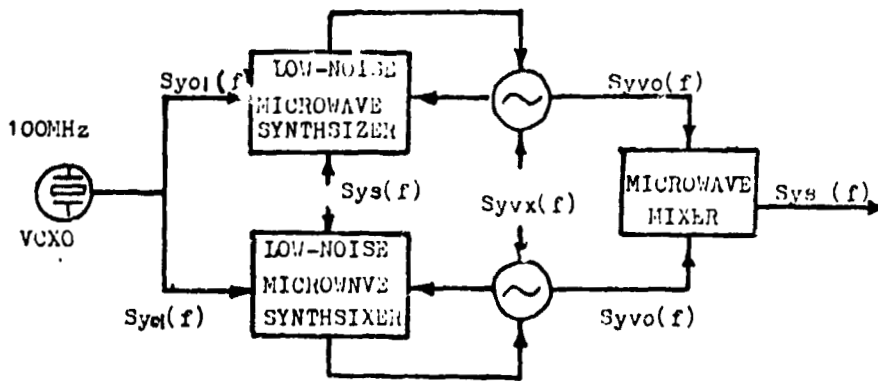
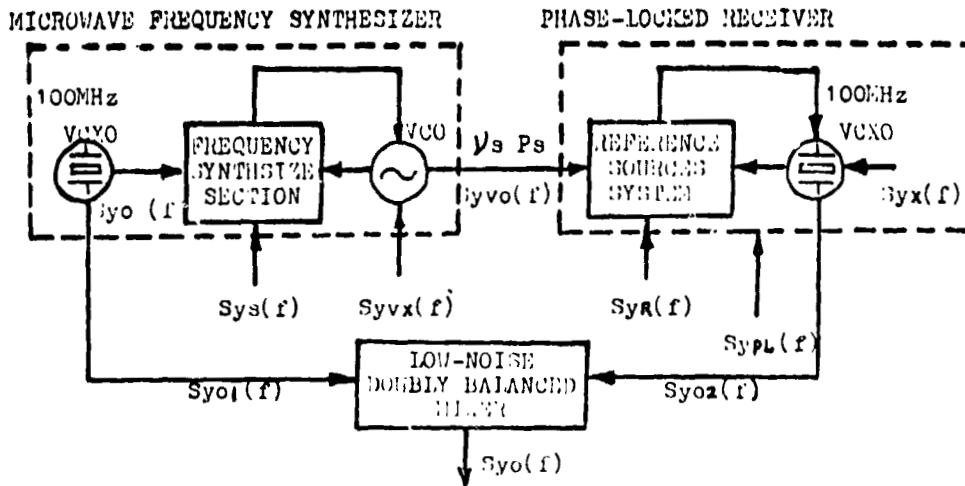


Fig.10. Actual tested time-domain frequency stability of PBR-II



ORIGINAL PAGE IS  
OF POOR QUALITY



(b)

Fig.12. Principle block diagram of Fig.11a, and Fig.11b.

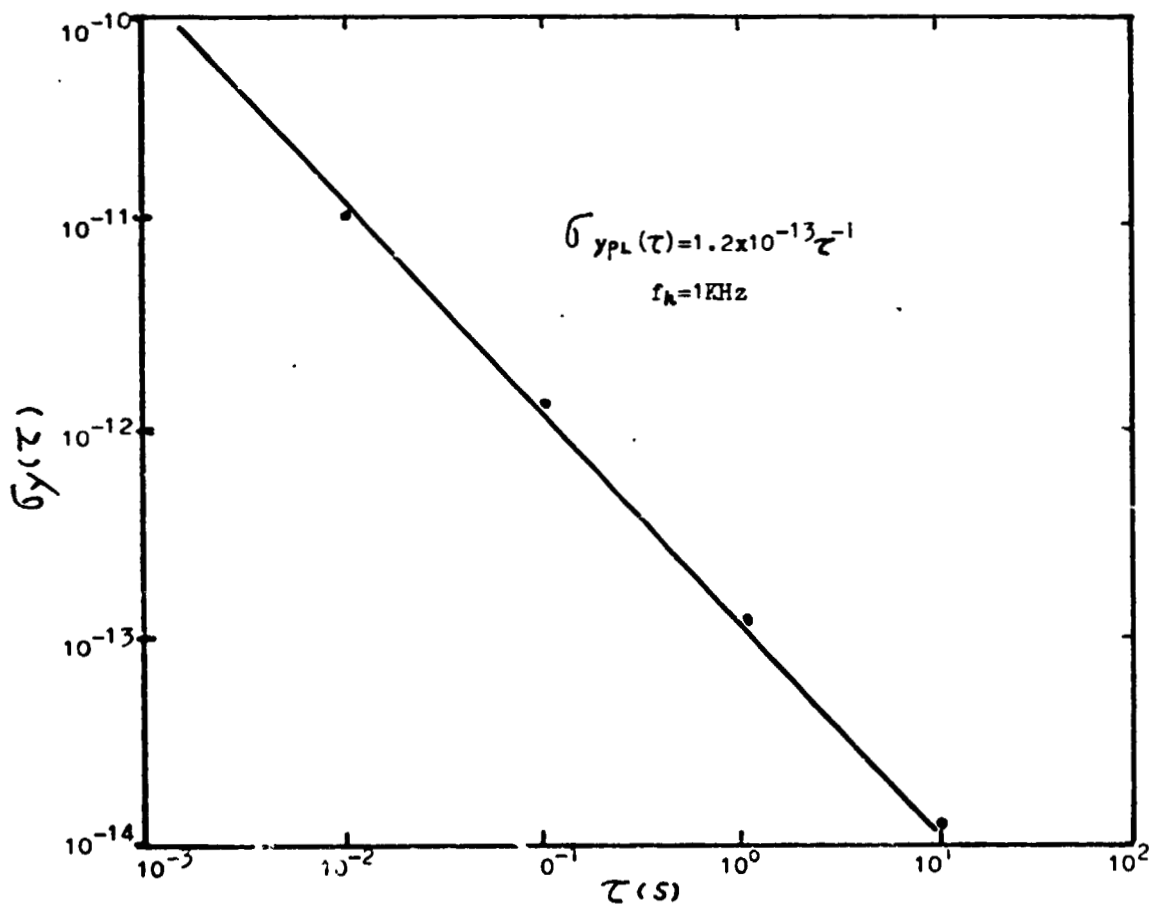


Fig.13. Phase-locked receiver noise contributions measured in the time-domain for  $f_k=1\text{KHz}$ .

ORIGINAL DOCUMENTS  
OF POOR QUALITY

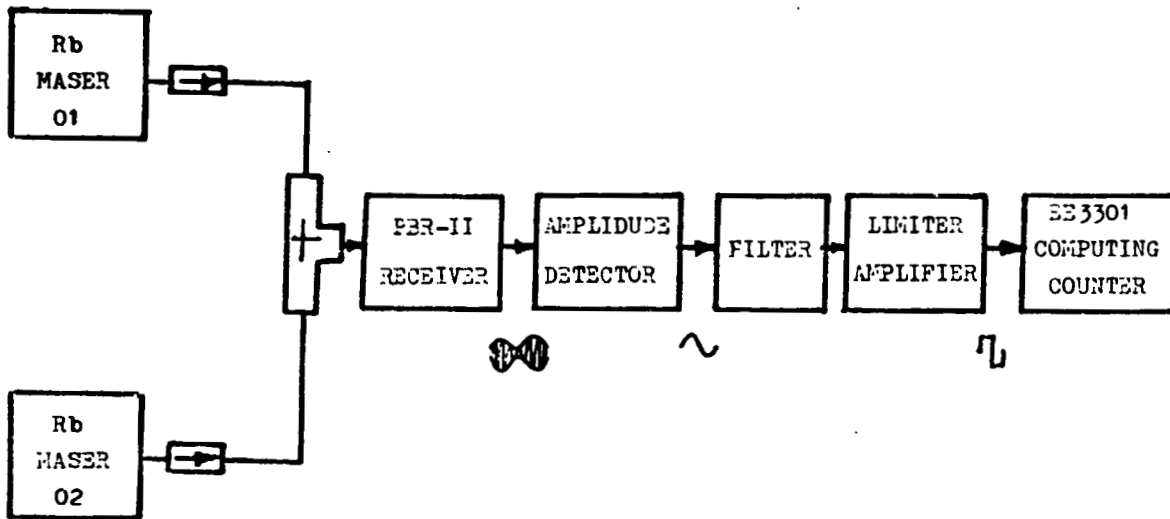


Fig.14. Block diagram of measurements Rb maser frequency stability.

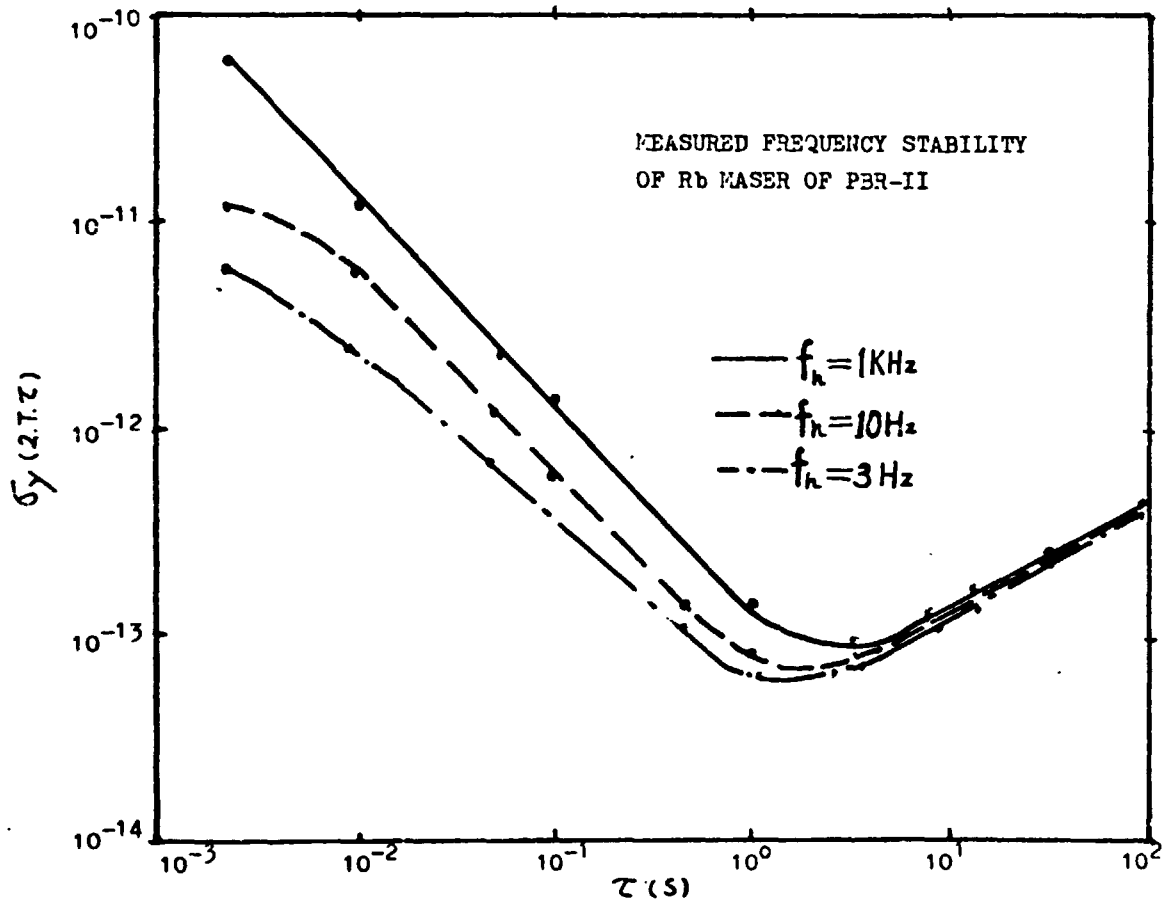


Fig.15. Time-domain frequency stability of Rb maser.

ORIGINAL PAGE IS  
OF POOR QUALITY

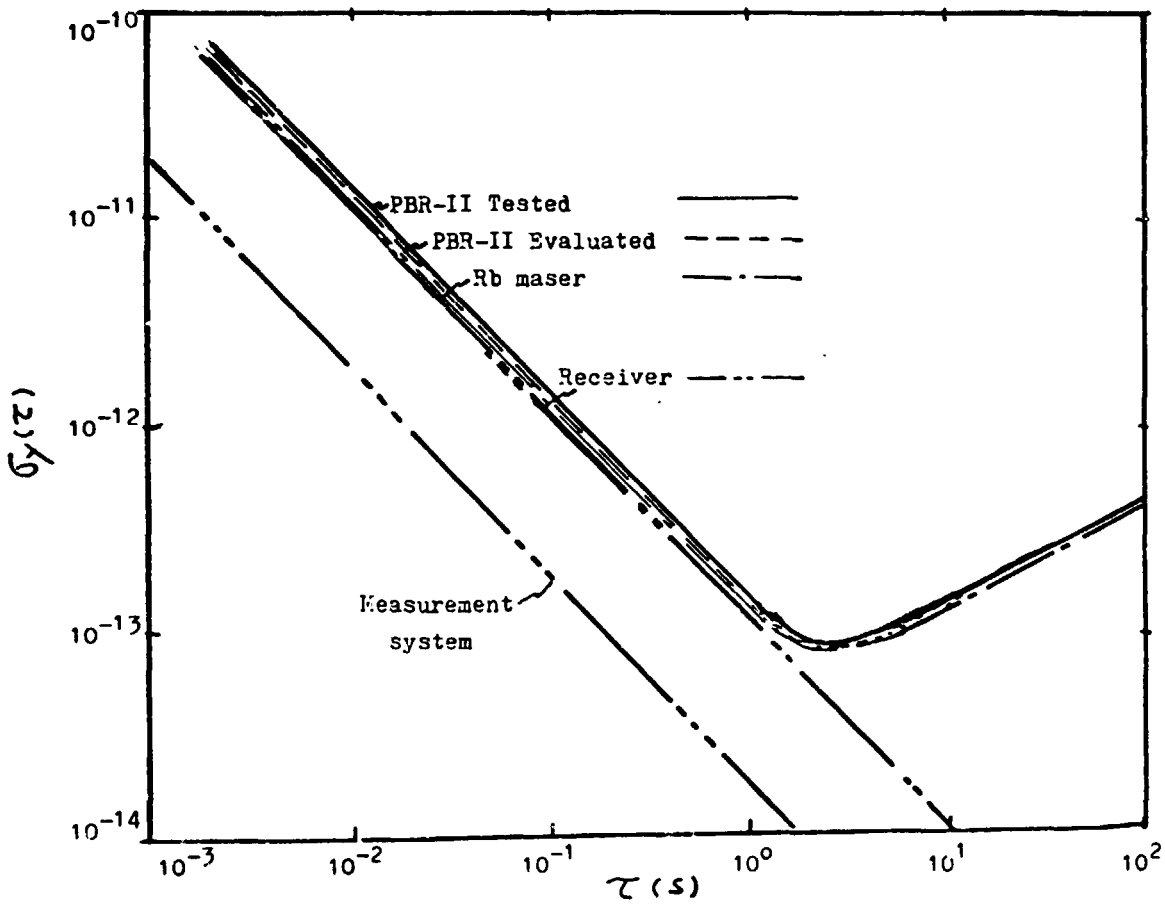


Fig. 16. Time-domain frequency stability

ORIGINAL PAGE 18  
OF POOR QUALITY

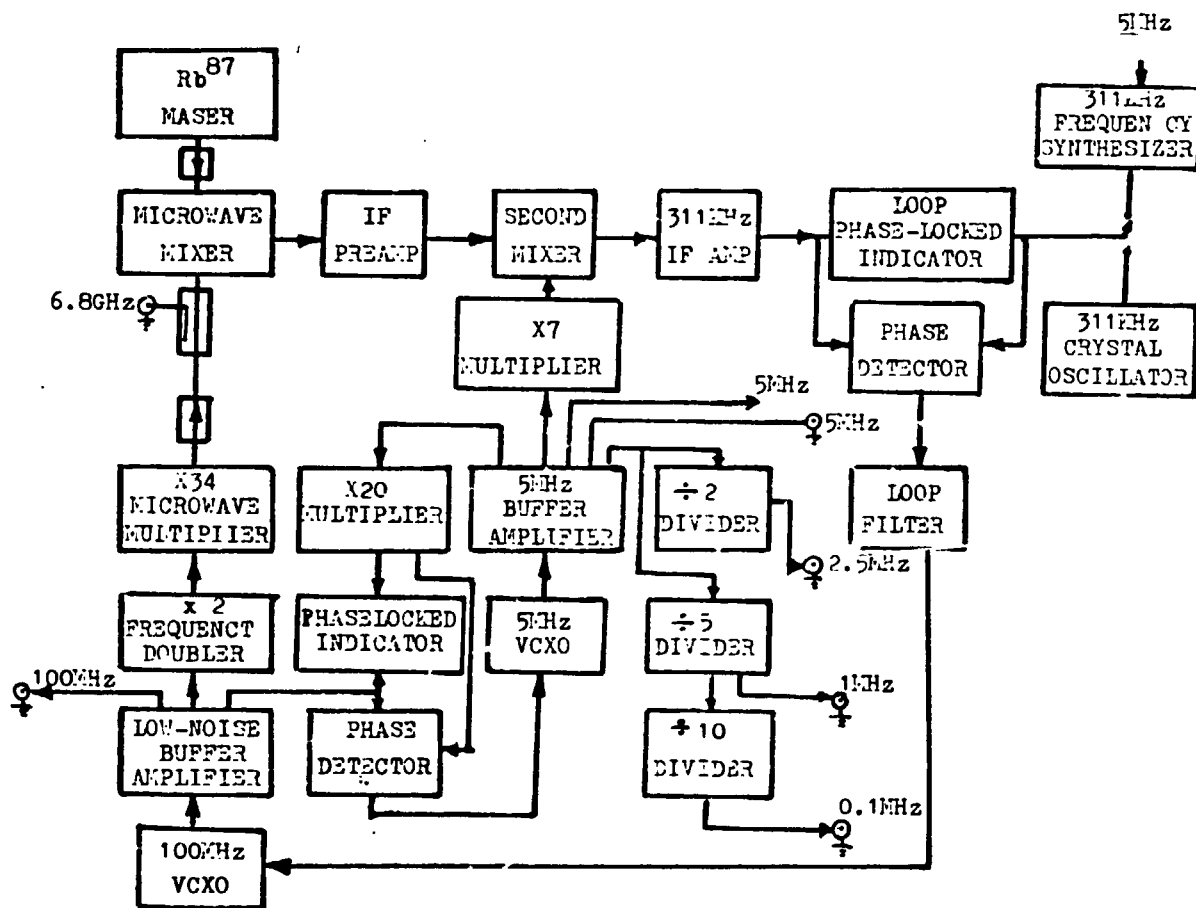


Fig.17. Detailed block diagram of PBR-II Rb maser frequency standard